Jet thrust vectoring using a miniature fluidic oscillator

G. Raman and S. Packiarajan
Dept of Mechanical, Materials and Aerospace Engineering
Illinois Institute of Technology, Chicago
USA

G. Papadopoulos and C. Weissman
Dantec Dynamics
Ramsey, NJ
USA

S. Raghu
Advanced Fluidics
Ellicot City, MD
USA

ABSTRACT

This paper presents a new approach to vectoring jet thrust using a miniature fluidic actuator that provided spatially distributed mass addition. The fluidic actuators used had no moving parts and produced oscillatory flow with a square wave form at frequencies up to 1·6kHz. A subsonic jet with an exit diameter of 3·81cm was controlled using single and dual fluidic actuators, each with an equivalent circular diameter of 1·06mm. The fluidic nozzle was operated at pressures between 20·68 and 165·47kPa. The objectives of the present work included documentation of the actuation characteristics of fluidic devices, assessment of the effectiveness of fluidic devices for jet thrust vectoring, and evaluation of mass flow requirements for vectoring under various conditions. Measurements were made in the flow field using a pitot probe for the vectored and unvectored cases. Some acoustic measurements were made using microphones in the near-field and for selected cases particle image velocimetry (PIV) measurements were made. Thrust vectoring was obtained in low speed jets by momentum effects with fluidic device mass flow rates of only 2×10^{-4}kg/sec (0·6% of main jet mass flow per fluidic oscillator). Although a single fluidic device produced vectoring of the primary jet, the dual fluidic device configuration (with two fluidic devices on either side of the jet exit) produced mass flux enhancement of 28% with no vectoring. Our results indicate that fluidic actuators have the potential for use in thrust vectoring, flow mixing and industrial flow deflection applications.

1.0 INTRODUCTION

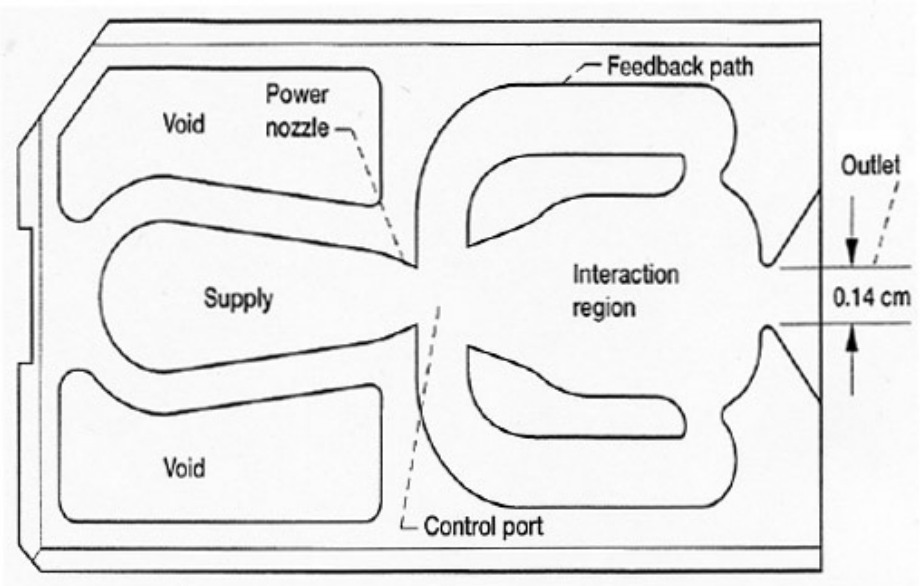
Thrust vectoring is of importance to aerospace vehicles and enables them to: (a) follow a desired flight path by changing the direction of the thrust vector in the propulsion device and (b) produce the required moments for attitude control of the vehicle. The conventional methods of using control surfaces for producing the forces and moments increase the component drag of the vehicle and hence thrust vectoring is an alternate method of achieving the same goal with minimum drag penalty. Two commonly used methods of thrust vectoring are mechanical vectoring by turning the entire jet exit area in the desired direction or by using a secondary source of fluid to direct the jet in the desired direction commonly known as fluidic jet vectoring. The main advantage of fluidic thrust vectoring is a significant reduction in the weight of the aerospace vehicle as well as fewer actuator parts for thrust vector control.

Although a substantial amount of work has been done on fluidic jet vectoring[1-4], the implementation of these actuation methods in full scale models have not been easy because of increased complexity of integrating these systems. The mechanisms and energy to produce large mass flow rates required, the electronic and mechanical systems associated with such actuators render these methods difficult for integration into many practical systems.

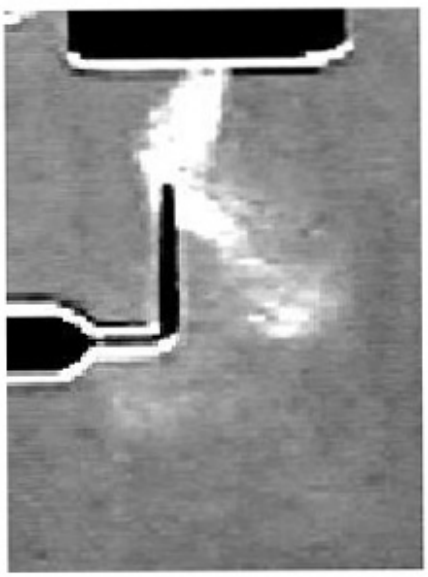
In this paper we describe the use of miniature fluidic actuators with no moving parts to obtain thrust vectoring. The main merit of this work is

Paper No. 2835. Manuscript received 18 March 2003 revised version received 22 July 2004 accepted 29 October 2004.

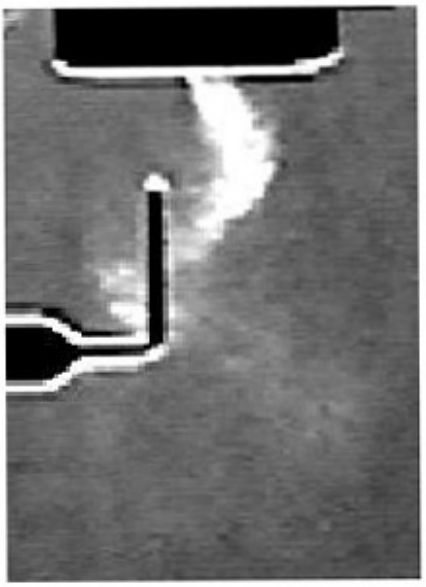
https://doi.org/10.1017/S0001924000000634 Published online by Cambridge University Press



(a)



(b)



(c)

Figure 1. Internal structure and operation of a miniature fluidic nozzle.
(a) Schematic diagram. (b) and (c) Schlieren images of the two phases of oscillation of a fluidic nozzle (courtesy of Prof. Sullivan, Purdue University, Sakaue *et al*[17]).

https://doi.org/10.1017/S0001924000000634 Published online by Cambridge University Press

the demonstration of new fluidics technology that distributes mass and injects perturbations at prescribed frequencies to bring about thrust vectoring. The present configuration has not been optimized for aircraft main jet vectoring and a number of issues such as actuator location and scalability need to be addressed before its use.

The field of fluidics evolved in the 1960s to meet the demands of robust and reliable logic elements in control systems. A number of fluidic devices such as turbulence amplifiers, wall attachment devices, active and passive momentum interaction devices, and vortex devices were developed primarily during the 1960s to perform many logic functions[5]. A common aspect of these fluidic devices is that a small auxiliary or 'control' jet is used as a momentum source to obtain large deflections in a 'power' or 'supply' jet. The application of such fluidic effects and devices as actuators for flow control in large systems such as a jet engine or a rocket nozzle exhaust has not been explored to the fullest extent.

In the 1970s fluidic control techniques were applied to a jet nozzle by Hermann Viets[6] who referred to this device as a flip-flop nozzle. Experiments at NASA Glenn extended the operation of flip-flop nozzles to supersonic speeds[7]. Raman *et al* (1994)[8] first evaluated the potential for their use as excitation devices and then applied such devices for jet mixing control[9-11]. It should be noted that one disadvantage of the Viets type of devices was that they were quite bulky, oscillated at frequencies less than 500Hz, consumed considerable mass flow and posed difficulties when they had to be integrated into a functioning practical device. However, with advances in miniaturization and microfabrication techniques there is now the ability to integrate these microfluidic devices into the body of nozzles or aerodynamic surfaces with minimal obtrusiveness. Raman *et al* (1999)[12] used such miniature (1-2mm) fluidic actuators to suppress cavity resonance. The fluidic actuator had all feedback passages built into the nozzle body. The fluidic devices used in the present study were invented, designed and fabricated at Bowles Fluidics Corporation[13-14].

Fluidic excitation devices are potentially useful for shear flow control for several reasons: they have no moving parts, they can produce excitation that is controllable in frequency, amplitude and phase, they can operate in harsh thermal environments, are not susceptible to electromagnetic interference, and are easy to integrate into a functioning device.

2.0 FLUIDIC OSCILLATORS

Most of the fluidic actuators produce an oscillating jet at the exit of the device. The oscillations are produced by the internal switching of a jet by a feedback mechanism. Figure 1(a) shows the internal structure of a miniature fluidic nozzle developed by Bowles Fluidics. A jet of fluid attaches to one of the two sides of a surface due to the 'wall attachment', commonly known as the 'Coanda' effect. The pressure distribution in the cavity is accordingly changed and the feedback channel transmits this pressure differential back to the point of the jet separation thus deflecting the jet to the other side. This cycle is repeated on the other side of the cavity through the feedback channel thus producing an oscillating jet at the exit of the cavity. Thus, this device does not need external signals or actuation to produce oscillating jets. Frequencies from 1-10kHz have been obtained with meso scale (nozzle sizes in the range of 200 microns –1mm) fluidic actuators with very low mass flow rates of the order of (10^{-3}kg/sec, see Ref. 14). More recently fluidic devices with simpler internal geometry (no feedback paths) which produce very high frequency (5-10kHz) oscillating jets have been developed[15]. Note that such innovative methods of pulsing or oscillating jets are very attractive in comparison to conventional methods using rotating valves.

Two phases of the oscillatory jet produced using the feedback type device (employed in the present work) are depicted in Figs 1(b) and 1(c) (Courtesy of Purdue University, Gregory *et al* (2004)[16]). The jet in the Schlieren pictures issues from top to bottom. The edge of the nozzle is seen as a black strip at the top and the jet, represented by a white lobe, is seen to be oscillating from side to side. The hot-wire probe in the foreground was used by Sakaue *et al* (2001)[17] to make unsteady velocity measurements.

In this paper, some detailed characteristics of fluidic actuators are first discussed and then the use of such actuators for thrust vector control and jet mixing enhancement is demonstrated.

3.0 EXPERIMENTAL TECHNIQUES

Several measurement techniques were used in this study. The oscillatory near-field hydrodynamic pressures of the fluidic actuator were measured using a Bruel and Kjaer 0·635cm microphone. Detailed flow field data was acquired using PIV and a pitot probe. The PIV technique was used in the present study because of its intrinsic advantage compared to LDV or hot-wire anemometer techniques for the present experimental geometry (1mm jet oscillating at 2-10kHz). The volume flow through the fluidic actuators was measured using mini-rotameters and the calculated densities were used to estimate the mass flux. Experimental details are provided only for the PIV technique and not for the other conventional techniques.

4.0 PIV SYSTEM AND DATA ANALYSIS

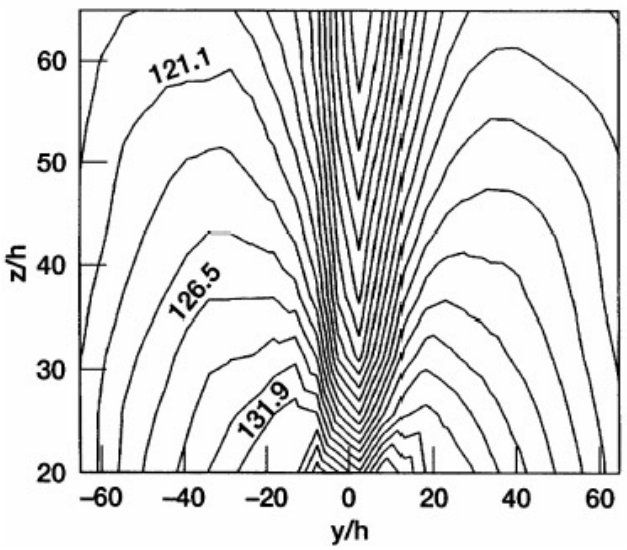
A commercial (Dantec Dynamics) PIV system was used consisting of a laser illumination source, digital imaging device, and dedicated hardware and software for data analysis. The illumination source was a frequency-doubled, double-cavity Nd:YAG laser operating at a wavelength of 532nm (50mJ per pulse) and a pulse rate of 15Hz. The overlapped core beams were expanded into a 20° diverging light sheet using focusable sheet-forming optics. At the measurement station, the sheet was approximately 1mm thick and illuminated a vertical diametric plane at the jet exit. Recording of particle image pairs was accomplished via an 8-bit double-frame CCD camera having a resolution of 1018 × 1018 pixels. This type of camera eliminated image order ambiguity and allowed for the use of cross-correlation methods when determining velocity vectors. A band-pass filter centered at 532nm (±15nm) was placed in front of the camera lens to negate white light illumination effects on the acquired images. Processing of the images to derive vector maps was done on-line using a second-order accurate adaptive cross-correlation technique. This is a multi-pass algorithm whereby velocity information from previous steps are used to improve vector displacement estimates on future steps that utilise increasingly smaller interrogation areas, thus increasing resolution of velocity gradients without compromising dynamic range and signal-to-noise performance. Setting of data acquisition parameters and management of data was accomplished using dedicated software to interact with a programmable processor, which housed an advanced synchronisation module for accurate control of laser and camera timing sequences.

Seeding of the jet was accomplished using a water atomiser, which produced approximately 1- to 2-μm size droplets. For each measurement, 150 recordings were collected to evaluate mean velocity characteristics. The time separation between pulses was set so as to yield maximum particle displacements of 20% to 25% of the initial 64 × 64 pixel interrogation area length. A final interrogation area of 16 × 16 pixels was chosen. A peak-validation and moving average technique[18]) was used to invalidate erroneous vectors at each step of the calculation procedure.

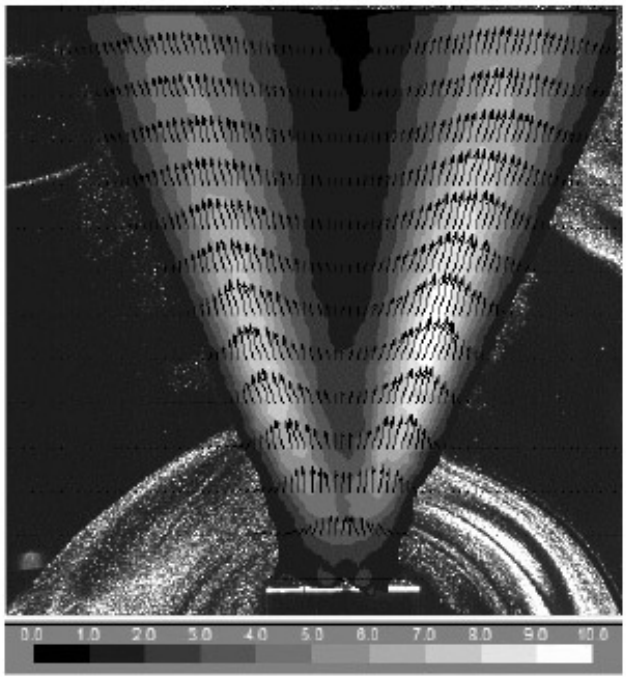
5.0 FLOW FIELD CHARACTERISTICS OF THE FLUIDIC ACTUATORS

Figure 2(a,b) shows a detailed time averaged dynamic pressure map and PIV image of the flow from a miniature fluidic nozzle. Relative to the fluidic actuator '*z*' and '*y*' represent the vertical and transverse

https://doi.org/10.1017/S0001924000000634 Published online by Cambridge University Press



(a)



(b)

Figure 2. Nearfield pressure and velocity characteristics of a miniature fluidic nozzle. (a) nearfield pressure map measured using a microphone. (b) instantaneous velocity map measured using PIV.

coordinates, respectively. The dynamic pressure measurements were made by traversing a 0·635cm microphone over the entire near-field of the fluidic nozzle (see Fig. 2(a)). Note that locations closer than z/h = 20 were not covered because of possible damage to the expensive microphone sensors. The sound pressure levels were in the range from 132 to 121dB over the z/h range from 20 to 60. The dual lobe nature of the dynamic pressure field is caused by the oscillatory jet that has longer dwell times at the extreme positions of the jet. Figure 2(b) shows the time averaged PIV data taken on the miniature fluidic nozzle. A TSI atomiser was used to inject seed particles through the 1mm actuator nozzle. The entire jet (fluidic control jet) was impregnated with seed particles. There were considerable difficulties in seeding and the resulting flow sometimes consisted of spurts of fluid followed by low levels of seed particles. After numerous trials data was taken for a few cases. The time averaged data gives us an idea of the magnitude, direction and distribution of velocity perturbations that were obtained using the fluidic actuator. It is also to be mentioned that the angle of the jet spread can be varied by appropriate design modifications in the fluidic device[12].

Figure 3 provides data on the frequency (f) and sound pressure level (SPL) produced by a miniature fluidic oscillator. The frequency data indicate that the fluidic actuator could produce oscillations at frequencies as high as 1,600Hz. The amplitude data indicates levels as high as 118dB. However, the amplitude data is very location dependent. Microphone locations are provided in the figure captions and will not be repeated herein. An entire map such as that shown in Fig. 2(a) is required to characterise the amplitude of such actuators at each pressure level. Spectra at various pressures are given in Fig. 3(a-c). The fluidic actuator used is of the bi-stable type with increased dwell at the extreme locations and a rapid switch between the two extremes. The primary frequency at which the flow from the fluidic device oscillates is the lowest frequency observed in the spectrum. In addition to this primary frequency several harmonics are also observed in the spectrum which is what one would expect in the case of a bi-stable oscillator.

6.0 EXPERIMENTS ON THRUST VECTORING

Figure 4 shows a schematic depicting the experimental setup and the relative dimensions of the main nozzle and the fluidic actuators. The primary jet used in the present work was a 3·81cm diameter circular jet. A single fluidic actuator was mounted near the top of the primary jet as shown in the figure. The exit dimensions of the fluidic actuator nozzle were 1·7mm × 0·95mm and was oriented, using installation fixtures, to obtain transverse injection into the primary jet. For a limited set of experiments another fluidic device was located symmetrically at the bottom of the primary jet. The flow from the actuator was normal to that of the primary jet. The velocities of the primary jet and the actuator could be controlled independently. A pitot probe was used to survey the entire flow field with and without fluidic actuation. A light delivery system fitted with focusable optics and attached to the double cavity Nd:YAG laser was located downstream under the jet was used to produce the laser light sheet for the PIV measurements.

6.1 Centreline velocity decay and jet velocity profiles

Figure 5 shows jet centreline velocity data for various levels of fluidic excitation. As the fluidic actuator supply pressure measured at the supply line is increased from 0 to 165·47kPa. (gauge pressure) the jet centreline appears to decay more rapidly. One should note that the significant decay of jet centreline velocity as indicated in Fig. 5 is quite deceptive. One could easily misinterpret the data as being a significant reduction in jet centreline velocity (or jet mixing enhancement). Note that there is a modest decay of centreline velocity, although the primary effect is that the vectoring pushes the jet towards the floor of the room and the centreline velocity sensor is thus near the outer edge of the jet. Data are shown for excitation using single fluidic devices. Note that when dual fluidic jets are used, the effects are entirely different and will be discussed in a later section. Thus, the centreline velocity alone is not enough to distinguish between the two effects and this will be seen later through detailed flow-field data. In an effort to confirm that the vectoring

https://doi.org/10.1017/S0001924000000634 Published online by Cambridge University Press

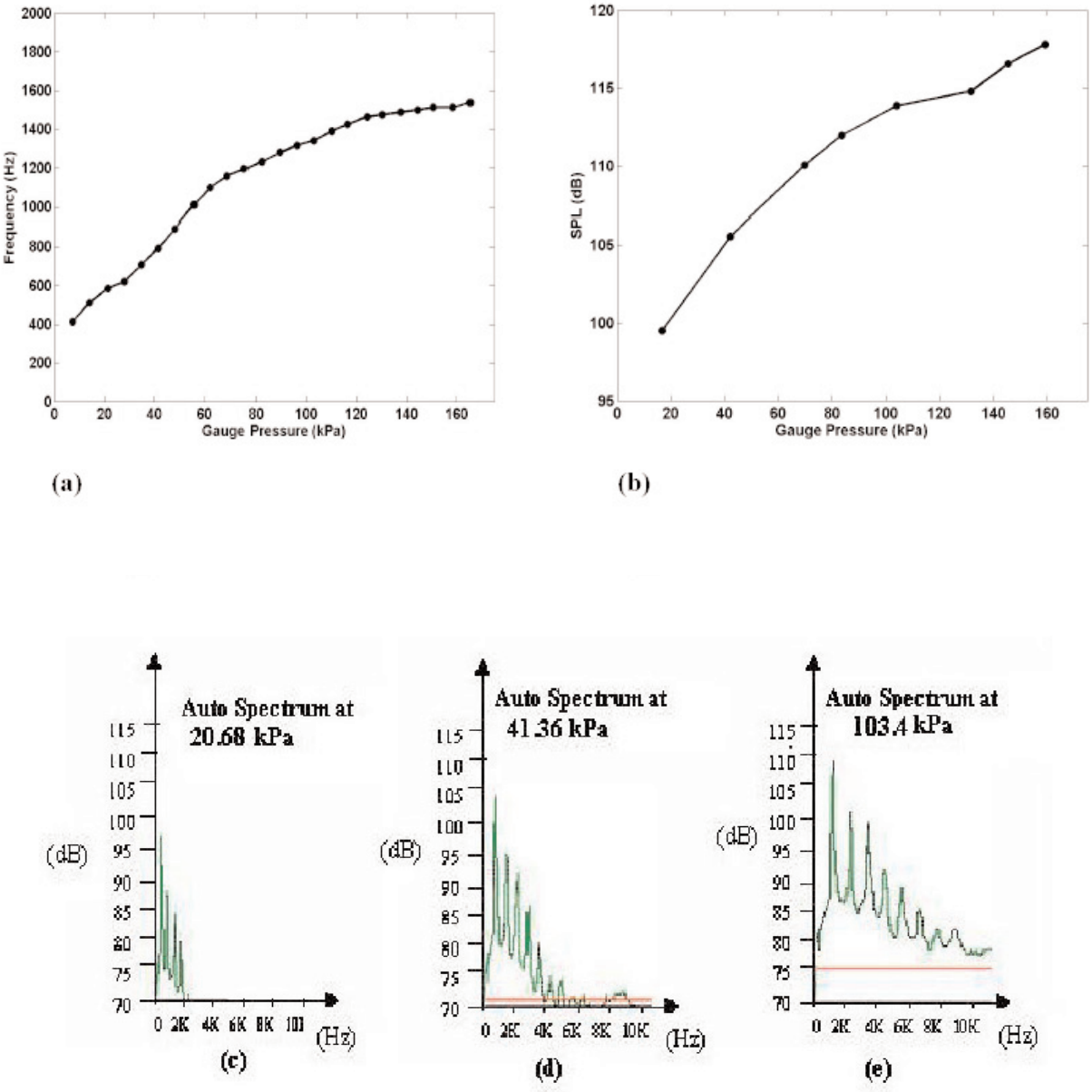


Figure 3. Frequency and amplitude characteristics of a miniature fluidic nozzle. (a) frequency and (b) sound pressure level, dB for various nozzle operating pressures. (c)-(e) spectral characteristics of the signal produced by miniature fluidic nozzles at various operating pressures.

effect cannot be obtained by the same amount of steady mass addition an equivalent mass flow circular nozzle (equivalent diameter = 1·34mm) was designed and tested. One can infer from the data shown in Fig. 5(b) that steady mass addition from an equivalent circular nozzle is not as effective as the addition of oscillatory mass (2·04 *E* –4kg/sec) through a fluidic nozzle. Velocity profiles taken across the jet confirm that the jet is indeed being vectored (see Fig. 6, 'radial velocity profiles') for the case when a single fluidic was used. This was also confirmed by measurements made over entire cross sectional planes. Note that in, both Figs 5(a) and 6, there is a distinct jump in effectiveness of the injection between 103kPa and 124kPa. A closer examination of the frequency and amplitude data of Figs 3(a) and 3(b) do not offer any further clarifications for this jump.

6.2 PIV measurements

PIV data are shown in Fig. 7(a-c) for the unperturbed case and for two cases of fluidic actuation. The figure shows the time averaged mean velocity field of issuing jet from 150 PIV realisations, overlaid

https://doi.org/10.1017/S0001924000000634 Published online by Cambridge University Press

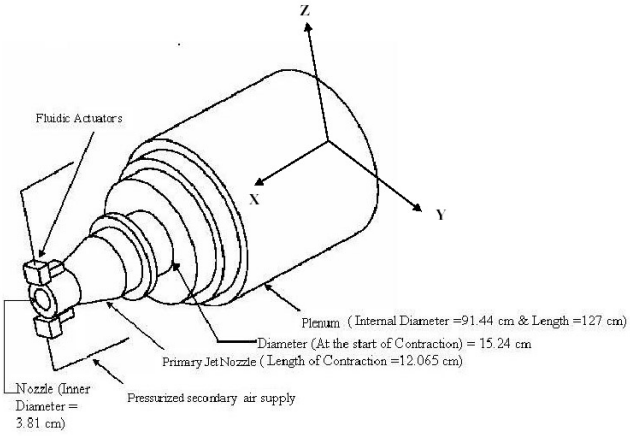


Figure 4. Schematic of primary jet with fluidic actuators and coordinate axes setup.

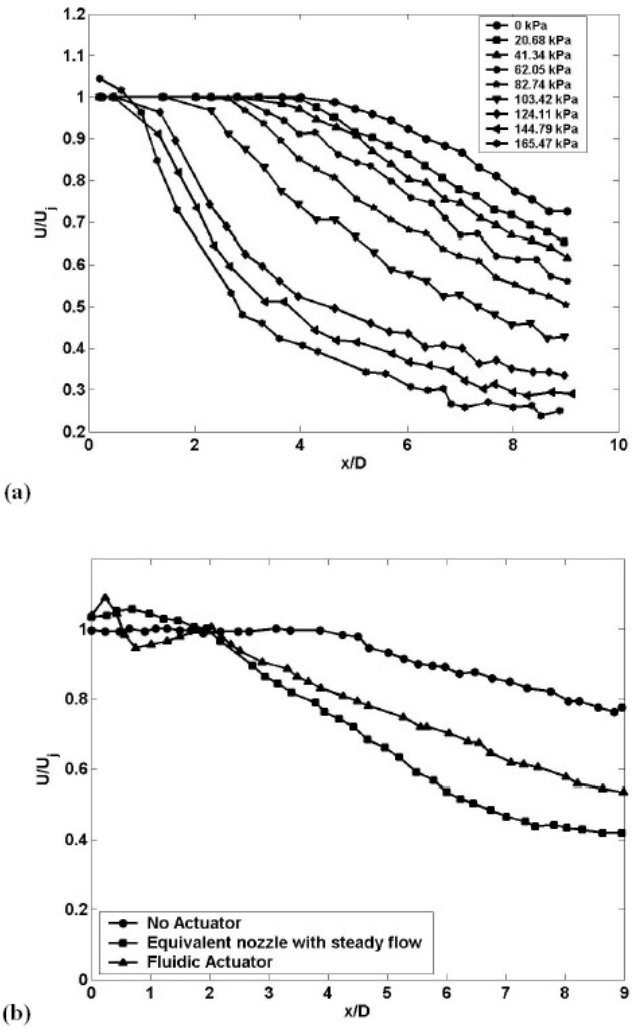


Figure 5. Jet centreline velocity distributions.
Plenum pressure = 344·73Pa, jet exit velocity = 24ms^{-1}.
(a) single fluidic actuator (b) comparison with steady blowing.

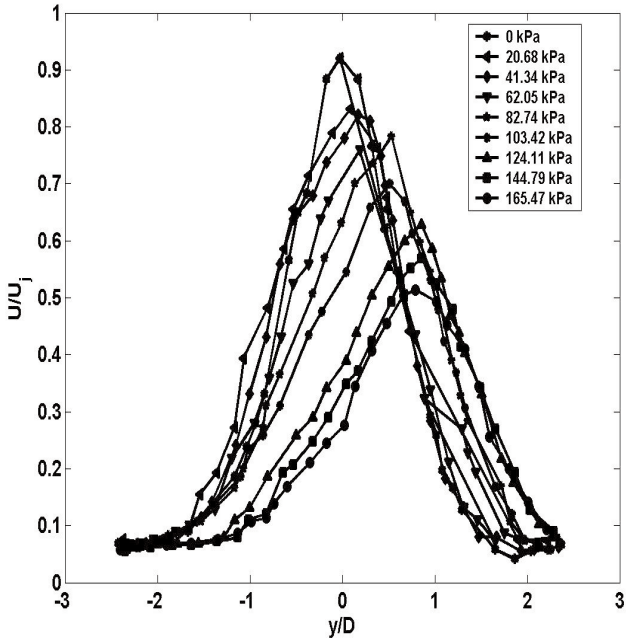


Figure 6. Radial velocity profiles showing thrust vectoring for various levels of fluidic actuation. Primary jet plenum pressure = 344·73Pa, jet velocity = 24ms^{-1}.

on an image of the seeded flow obtained by the laser sheet flow visualisation for the cases (a) no actuation; (b) single actuator operating at 20·68kPa (gauge pressure); (c) single actuator operating at 62·04kPa (gauge pressure). The contour levels denote magnitude of the velocity field in ms^{-1}. With the fluidic actuator on at the top of the main nozzle, the jet is vectored downwards. For a supply pressure of 20·68kPa (mass flow = 2 × 10^{-4} kg/s or 0·6% of the main jet mass flow) to the fluidic actuator, a jet deflection of about 5° is seen from the data. The deflection increased with the increase in the supply pressure to the fluidic actuator and with a supply pressure of 62·04kPa (mass flow = 5·39 × 10^{-5} kgs^{-1} or 1·62% of the main jet flow), a deflection of about 15° was obtained. It is observed that the deflection angle of the jet does not vary linearly with either the pressure or the mass flow rates.

The time averaged streamlines and the vorticity fields for the three cases (a) no actuation; (b) single actuator operating at 20·68kPa; (c) single actuator operating at 62·04kPa are shown in Fig. 8. From the direction of the streamlines, we can see that the jet is deflected by about 5 degrees for 20·68kPa actuation pressure and about 10° for 62·04kPa actuation pressure.

The vorticity contour is symmetric for the case of no actuation and becomes asymmetric with fluidic actuation. The maximum vorticity occurs in the shear layer at the exit region of the jet. Further downstream, for the cases of fluidic actuation, the peak vorticity on the bottom side of the jet (opposite side of the actuator location) rapidly reduces in the downstream direction. The vorticity is also more diffused on the bottom side and the positive vorticity values (from the bottom shear layer) are seen extending much farther into the top shear layer indicating increased mixing.

6.3 Detailed flowfield measurements

Detailed velocity measurements using a hotwire in different planes of the jet are shown in Figs 9, 10 and 11 for the unperturbed jet, single fluidic actuation case and actuation using two fluidic devices. The data in Figs 9 and 10 are two longitudinal slices of the jet that are normal to each other. Figure 11 shows cross sectional mean velocity

https://doi.org/10.1017/S0001924000000634 Published online by Cambridge University Press

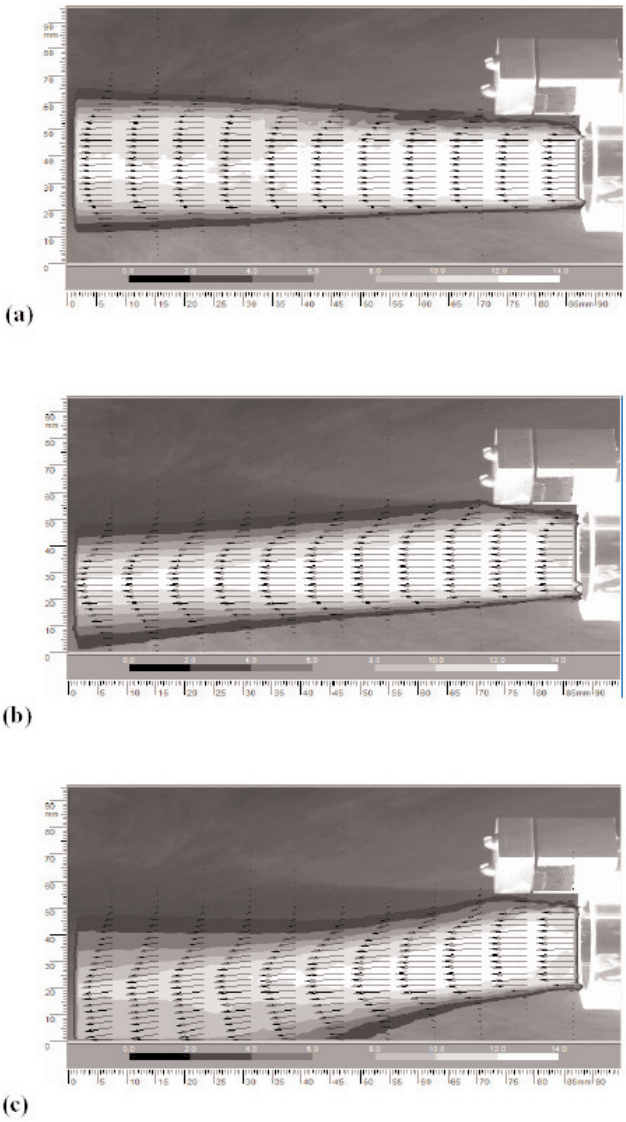


Figure 7. Time averaged velocity vectors obtained using PIV for various levels of fluidic actuation. Jet issues from right to left. Primary jet plenum pressure = 137·9Pa, jet exit velocity = 15ms^{-1} (a) no actuation. (b) single fluidic actuator operating at 20·68kPa. (c) single fluidic actuator operating at 62·04kPa.

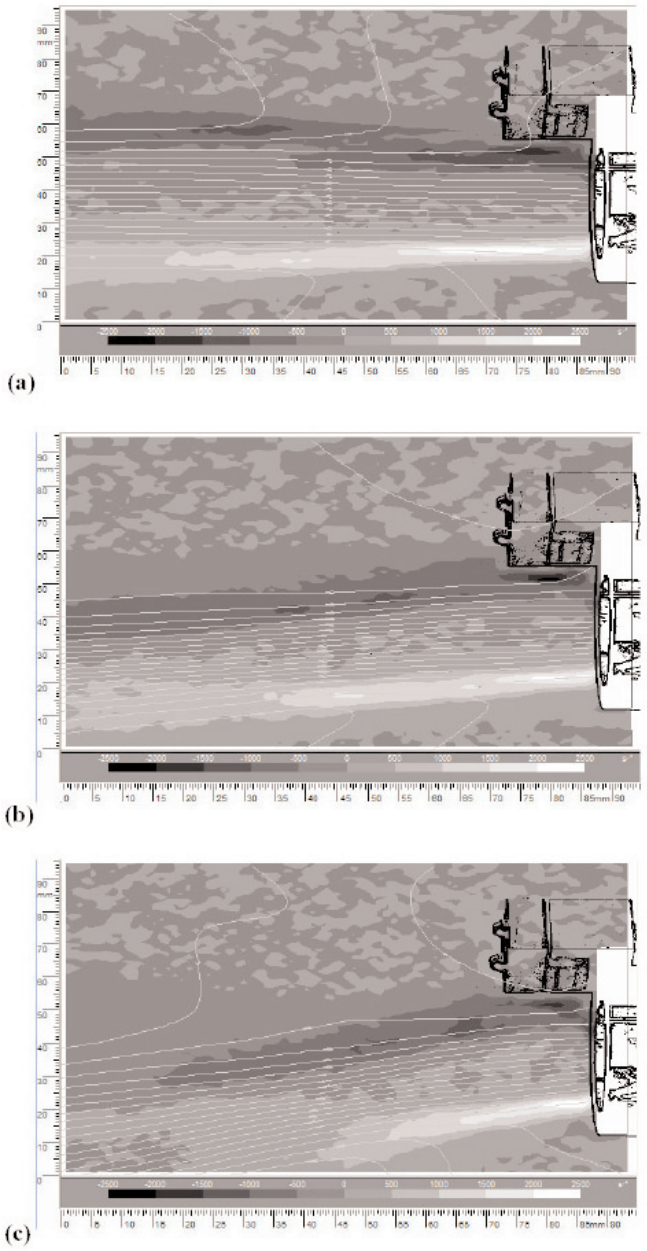


Figure 8. Vorticity and streamlines for various levels of fluidic actuation (parts (a)-(c)) correspond to those in Fig. 7.

data at x/D = 3, 6, and 9. It is important to recognise here the orientation of the measurement planes and the location of the fluidic actuator(s). The reader is referred back to the sketch in Fig. 4. Figures 9 and 10 represent vertical and horizontal slices of the data shown in Fig. 11. It is seen that the single fluidic actuator vectors the jet to the right in Fig. 11 (middle row). In contrast, the dual actuator case splits the jet into two parts. Figures 9-11 taken together provide a picture of the effect of single and dual actuators. In our work the thrust vectoring appears to be effected by momentum effects. Oscillatory and distributed mass addition works better than steady equivalent mass addition from a single miniature nozzle. In contrast to other methods that use co-flow or counter-flow[1] along with a Coanda surface and vector the main jet towards the direction where the actuation is applied our technique relies on momentum effects and vectors the main jet away from the actuation location. Note that using the counter-flow method the primary jet could attach itself to the Coanda surface. In contrast, our technique allows for an easy reversal of the vectoring effect. Based on the actuation frequencies and mass flow rates used it is clear that shear layer dynamics and interaction of the fluidic actuation frequency plays a secondary role as compared to the distributed momentum effects.

The mass flux ratio (the mass flux at a given axial location normalized by the mass flux at the exit of the main jet) was calculated for the cases shown in Fig. 11. Note that the measured mass flow through the fluidic device alone ranged from 1·18 × 10^{-4} to 5·41 × 10^{-3}kg/sec for supply pressures of 68·93psig to 206·8kPa,

https://doi.org/10.1017/S0001924000000634 Published online by Cambridge University Press

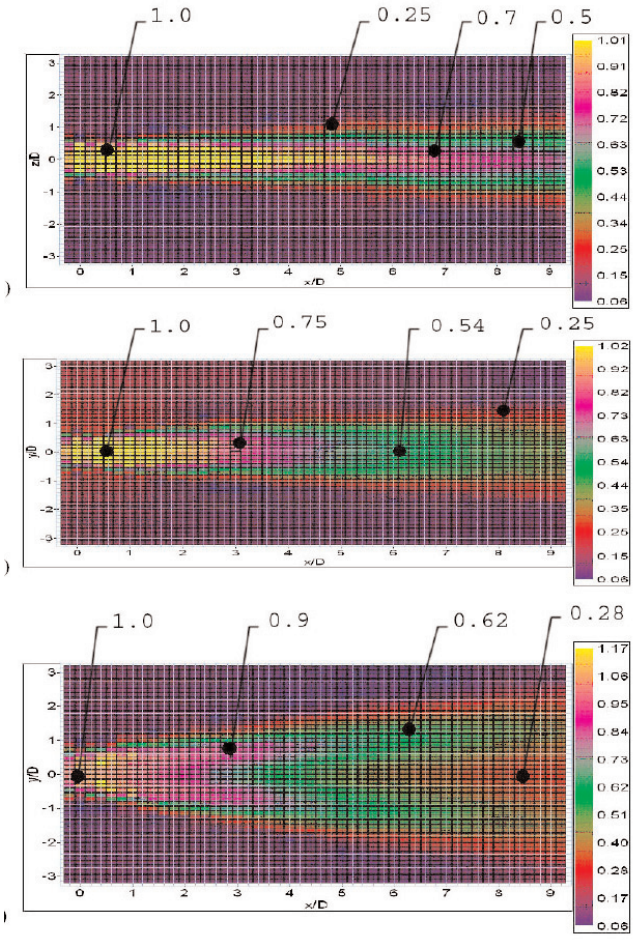


Figure 9. Normalised velocity distributions on the *xy* plane ($z = 0$). Primary jet plenum pressure = 344·73Pa, jet velocity = 24ms^{-1}. Fluidic actuator operating at 103·4kPa. (mass flow = 2·07 x 10^{-4} kg/s). (a) primary jet without fluidic actuation. (b) single fluidic nozzle located at $x = 0$, $y = 0$, $z = +1·9$cm. (c) two fluidic actuators located at $x = 0$, $y = 0$, $z1 = +1·9$cm , $z2 = -1·9$cm.

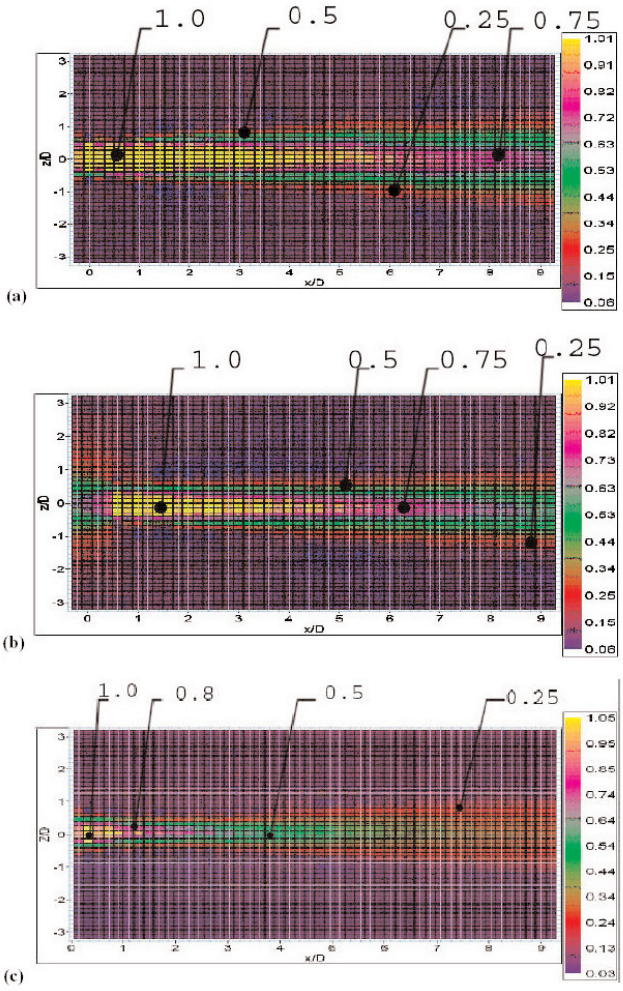


Figure 10. Normalised velocity distributions on the *xz* plane ($y = 0$). Other conditions the same as in Fig. 9.

respectively. For the single fluidic actuation case very little increase in mass flux of the main jet (calculated from cross-sectional velocity data) was recorded at $x/D = 3$, 6, and 9, and the effect of actuation was to vector the jet without changing the centreline velocity significantly. However, for the case with two fluidic actuators the mass flux was enhanced by 28% at $x/D = 9$ when compared to the unperturbed jet. The secondary mass added through the fluidic actuators was subtracted out for this calculation.

7.0 CONCLUSIONS

In this paper the use of miniature fluidic actuators that provide oscillatory and distributed mass addition for thrust vectoring has been demonstrated. The fluidic devices have no moving parts and have very low mass flow consumption (of the order of 2×10^{-4}kg/sec, or 0·6% of the main jet mass flow, at 103·4kPa). This demonstration was carried out at subsonic primary jet velocities. A single fluidic device was seen to vector the jet, whereas two fluidic devices located on either side of the jet nozzle enhanced mixing (mass flux) by about 28%. For the single fluidic actuator case, a comparison was made between the fluidic actuator and another that provided a steady mass injection into the primary jet using a circular nozzle of that had an equivalent exit area as that of the actuator. It was confirmed that steady mass injection did not affect the jet as much as the oscillatory fluidic excitation as far as changing the centreline velocity decay or the velocity profile are concerned. The potential for integrating miniature fluidic actuators to improve the performance of jet aircraft components and other applications requiring flow deflection or mixing enhancement has been demonstrated from the present experiments. The advantages of the fluidic actuators are that they do not have moving parts and that they can be fabricated using a variety of materials.

ACKNOWLEDGEMENT

The research reported in this paper was funded by the Illinois Institute of Technology's Educational and Research Initiative Fund (ERIF).

https://doi.org/10.1017/S0001924000000634 Published online by Cambridge University Press

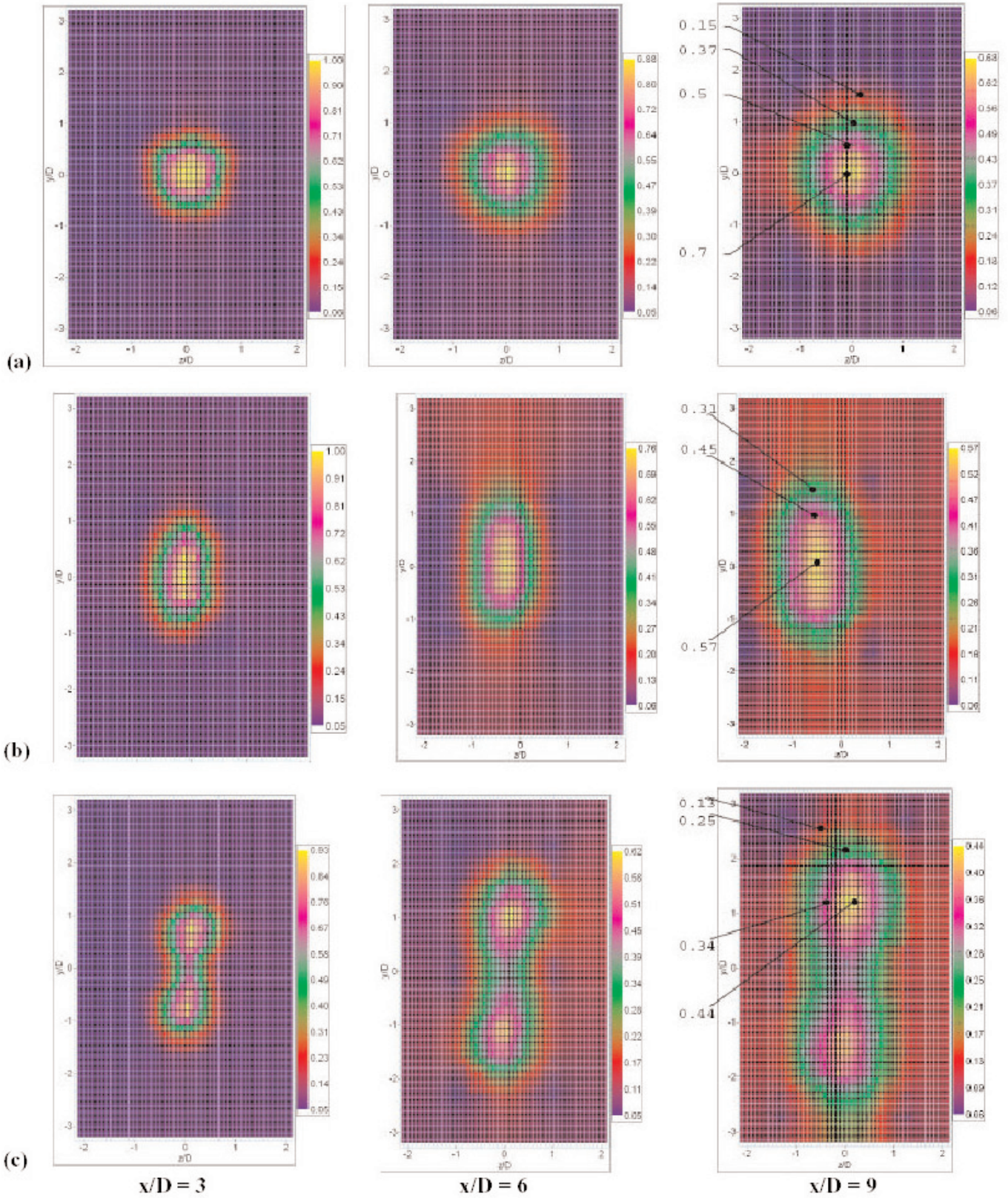


Figure 11. Normalised velocity distributions on the *yz* plane. (a) primary jet without fluidic actuation. (b) single fluidic nozzle located at $x = 0$, $y = 0$, $z = +1{\cdot}9$cm. (c) two fluidic actuators located at $x = 0$, $y = 0$, $z1 = +1{\cdot}9$cm, $z2 = -1{\cdot}9$ cm. Other conditions the same as in Fig. 9.

https://doi.org/10.1017/S0001924000000634 Published online by Cambridge University Press

REFERENCES

1. VAN DER VEER, M. and STRYKOWSKI, P.J. Counterflow thrust vector control of subsonic jets: continuous and bistable regimes, *J Propulsion and Power*, May-June 1997, **13**, (3).
2. SMITH, B.L. and GLEZER, A. Vectoring and small-scale motions effected in free shear flows using synthetic jet actuators, 1997, AIAA Paper 97-0213.
3. MILLER, D.N., YAGLE, P.J. and HAMSTRA, J.W. Fluidic throat skewing for thrust vectoring in fixed geometry nozzles, 1999, AIAA Paper 99-0365.
4. MASON, M.S. and CROWTHER, W.J. Fluidic thrust vectoring of low observable aircraft, 2002, CEAS Aerospace Aerodynamic Research Conference, Cambridge, UK, 10-12 June 2002.
5. MORRIS, N.M. *An Introduction to Fluid Logic*, 1973 McGraw Hill, UK.
6. VIETS, H. Flip-flop jet nozzle, *AIAA J,* 1975, **13**, pp 1375-1379.
7. RAMAN, G., HAILYE, M. and RICE, E.J. Flip-flop jet nozzle extended to supersonic flows, *AIAA J*, 1993, **31**, pp 1028-1035.
8. RAMAN, G., RICE, E.J. and CORNELIUS, D. Evaluation of flip-flop jet nozzles for use as practical excitation devices, *J Fluids Eng*, 1994, **116**, pp 508-515.
9. RAMAN, G. and CORNELIUS, D. Jet mixing control using excitation from miniature oscillating jets, *AIAA J*, 1995, **33**, pp 365-368.
10. RAMAN, G. and CORNELIUS, D. Multiple fluidic devices provide flow-mixing control, 1996, NASA Tech Briefs, Oct 1996, **20**, pp 91-92.
11. RAMAN, G. 1997 Using controlled unsteady fluid mass addition to enhance jet mixing, *AIAA J*, **35**, pp 647-656.
12. RAMAN, G., RAGHU, S. and BENCIC, T.J. Cavity resonance suppression using miniature fluidic oscillators, 1999, AIAA Paper 99-1900.
13. STOUFFER, R.D. 1985 Liquid oscillator device, US Patent 4508267.
14. RAGHU, S. and RAMAN, G. Miniature fluidic devices for flow control, 1999, ASME FEDSM 99-7256.
15. RAGHU, S. Feedback-free fluidic oscillator, 2001, US Patent 6253782.
16. GREGORY, J.W., SULLIVAN, J.P., RAMAN, G. and RAGHU, S. Characterization of a micro fluidic oscillator for flow control, 2004 AIAA Paper 2004-2692.
17. SAKAUE, H., GREGORY, J.W., SULLIVAN, J.P. and RAGHU, S. Porous pressure sensitive paint for unsteady flow details, 2001, AIAA paper 2001-0554.
18. MADSEN, A.H. and MCCLUSKEY, D.R. On the accuracy and reliability of PIV measurements, 1994, Seventh International Symposium on the Application of Laser Techniques to Fluid Mechanics, Lisbon, Portugal, 11-14 July 1994.

https://doi.org/10.1017/S0001924000000634 Published online by Cambridge University Press